

**A new method of surface resistance measurement with a niobium triaxial cavity working at 2 K**

Changnian Liang, Larry Phillips, and Ronald Sundelin

Citation: [Review of Scientific Instruments](#) **64**, 1937 (1993); doi: 10.1063/1.1143979

View online: <http://dx.doi.org/10.1063/1.1143979>

View Table of Contents: <http://scitation.aip.org/content/aip/journal/rsi/64/7?ver=pdfcov>

Published by the [AIP Publishing](#)

---

**GRANVILLE-PHILLIPS®**

ADVANCED VACUUM MEASUREMENT SOLUTIONS

Vacuum Gauges:

Convectron®, Micro-Ion®, Stabil-Ion®,  
Cold Cathode

Mass Spectrometers:

Vacuum Quality Monitors



[www.brooks.com](http://www.brooks.com)

Introducing the First  
Cold Cathode Gauge  
worthy of the  
**Granville-Phillips name!**

- Unsurpassed Accuracy
- Predictive & Easy Maintenance



# A new method of surface resistance measurement with a niobium triaxial cavity working at 2 K

Changnian Liang,<sup>a)</sup> Larry Phillips, and Ronald Sundelin

Continuous Electron Beam Accelerator Facility, 12000 Jefferson Avenue, Newport News, Virginia 23606

(Received 8 February 1993; accepted for publication 25 March 1993)

A 1.5-GHz superconducting niobium triaxial cavity has been fabricated to study residual surface resistance of superconducting materials at 2 K. Unlike many other structures where the entire test samples have to be placed in strong magnetic field locations, we have the edge of a 25.4 mm or larger diameter sample outside of the strong field region, a procedure which will greatly reduce edge effects and image current losses between the thin film and substrate. A calorimetric method is used to measure the sample losses, and is designed to resolve a 10- $\mu$ K temperature change using 16 carbon resistor sensors. A detection limit of 0.05- $\mu$ W power dissipation has been determined with a calibration heater, which corresponds to a surface resistance of 0.02 n $\Omega$  at a maximum cavity magnetic field of 250 G. Initial cavity testing was performed in a magnetically unshielded cryostat, yielding a 2.2- $\mu$  $\Omega$  residual resistance which was measured by both the rf measurement and the calorimetric measurement.

## I. INTRODUCTION

The rf cavity method has been widely used for microwave characterization of high  $T_c$  superconducting materials.<sup>1</sup> At high frequencies, copper cavities are frequently used because it is convenient to perform experiments at different temperatures and in high magnetic fields. In addition, rf losses in normal conductors are less sensitive to frequency than rf losses in superconductors ( $f^{1/2}$  vs  $f^2$ ). Superconducting cavities are usually employed for small crystal samples and high quality epitaxial thin films when high sensitivity is required. Among all the published results to date, a cylindrical cavity used in its TE<sub>011</sub> mode is one of the most popular choices due to the fact that there are no currents crossing indium vacuum sealing joints.<sup>2</sup> There are two ways to place a sample in a TE<sub>011</sub> cavity. One is the end plate replacement method, which replaces one end plate with a disk sample. Its resonant frequency is usually high due to the limited size of epitaxially grown samples. The other is the  $Q$ -perturbation method, which places the sample on the maximum magnetic field location within the cavity. The cavity dimension is not limited by the sample size, as the end plate method is, but the sensitivity of the sample measurement decreases with increasing cavity size. Therefore, its frequency is also well above the frequency range for most accelerator applications.

Delayen *et al.* developed a  $\lambda/4$  TEM cavity which has a resonant frequency of 820 MHz, which is within the most common range of accelerator frequencies of 0.3–3 GHz. It is more compact due to its coaxial line structure and more sensitive than the commonly used TE<sub>011</sub> cavity because the field is concentrated on the end plate with the center conductor.<sup>3</sup> Its strongest magnetic field location is at the joint of the center conductor and the bottom plate. A 24-mm-diam sample has been placed at the strongest magnetic field region to measure its surface resistance at 4.2 K. The

relationship between the surface resistance and the surface magnetic field has also been measured up to 300 G when the cavity is filled with liquid helium.

One disadvantage of the  $Q$ -perturbation method is that the entire sample has to be placed at the maximum magnetic field location for the sake of achieving highest sensitivity. This might result in some unwanted losses on the sample edge and between the interface of the thin film and the substrate,<sup>3</sup> or in the substrate itself. The thin-film quality at the edge is usually poor, and current flow across the entire sample requires image currents under the sample. Another disadvantage arising from this requirement is that the location of the sample usually breaks the cylindrical symmetry and the geometrical factor of the sample thus cannot be calculated accurately with URMEL<sup>4</sup> or SUPER-FISH,<sup>5</sup> a stainless steel or niobium sample calibration is always needed, which introduces another step contributing to the measurement error.

We have designed a 1.5-GHz superconducting triaxial niobium cavity working at 2 K. This frequency is chosen to be the same as that of the 4-GeV accelerator at CEBAF. By adopting a tapered cone structure, we can have the edge of a 25.4-mm-diam round sample outside of the strong magnetic field region, which will enable us to measure the intrinsic rf losses only on the top surface of the sample. We also applied a calorimetric method to measure the rf losses of the sample, using 16 carbon resistors as temperature sensors. The calorimetry method used measures rf losses of the sample alone and is able to exclude other losses caused by the niobium cavity, indium joints, coupling probes, and by field emission impacting at places other than the sample. The sensitivity of the sensors at 2 K is high, which enables us to measure a temperature change of 10  $\mu$ K. This corresponds to a resolution of 0.02-n $\Omega$  surface resistance at a field of 250 G, which makes our cavity sensitive enough to measure 25.4-mm-diam samples of any existing material.

We have tested the triaxial cavity at 2 K both by  $Q$  measurement and by calorimetry. The results from both

<sup>a)</sup>Also at Department of Physics, Virginia Polytechnic Institute and State University, Blacksburg, VA 24061.

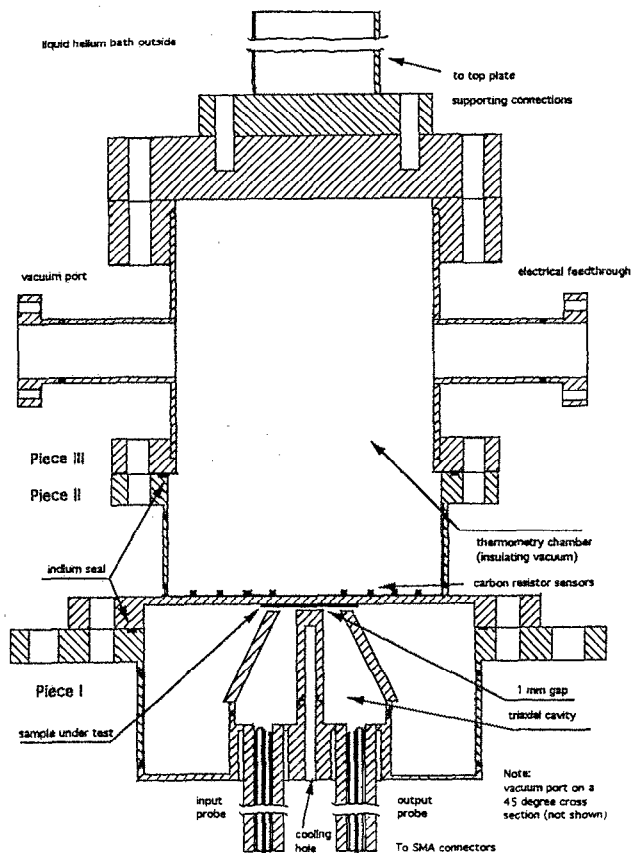


FIG. 1. The assembly consists of three pieces. Pieces I and II are made from reactor grade niobium, and Piece III from stainless steel. Vacuum port of the cavity is not shown.

methods agree well using a  $2.2\text{-}\mu\Omega$  residual resistance of niobium caused by trapped magnetic flux. The highest magnetic field in the cavity reaches 250 G, which is limited by the coupling probe for the moment. At a peak field of 95 G, the  $2.2\text{-}\mu\Omega$  surface resistance causes an rf loss of  $711\ \mu\text{W}$  on the top plate. The detection limit, obtained from our heater calibration, is  $0.05\ \mu\text{W}$ . This means our cavity has a sensitivity of  $0.02\ \text{n}\Omega$  at 250 G. In the following sections, we are going to describe our design, experimental procedure, and test results.

## II. CAVITY DESIGN AND FABRICATION

Figure 1 is a drawing of the niobium triaxial cavity and the vacuum chamber for calorimetric measurement. It consists of three separate pieces. Piece I is the bottom of the triaxial cavity, which consists of a center rod, a tapered cone, a cylindrical wall, two rf coupling ports, and one vacuum pumping port (not shown). Piece II is the cavity top plate, which completes the cavity and separates the cavity vacuum from the temperature sensor chamber vacuum. On the cavity side, a 25.4 mm or larger diameter thin-film sample can be put in the center for surface resistance measurement. On the other side of the plate, 16 temperature sensors are located on four concentric rings to measure the temperature distribution caused by rf losses on the sample when electromagnetic energy is stored in the

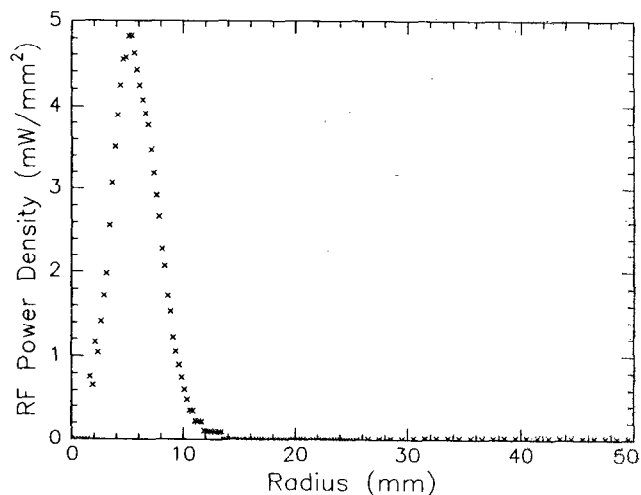


FIG. 2. Calculated power density distribution on the cavity top plate (Normalized to 1 W) from URMEL: there is negligible edge effect between 25.4 and 50 mm in diameter.

cavity. The plate provides a thermal resistance between the sample and the liquid-helium bath. Piece III is the other half of the temperature sensor chamber. Stainless steel is used because of the ease of machining and welding for vacuum ports and instrumentation feedthroughs. A 4 1/2-in. Conflat™ flange is used at the top of the sensor chamber as the support of the overall cavity assembly, and is connected to the top plate of the cryostat by a 1 1/2-in. stainless-steel tube. Piece II is made from reactor grade niobium because it has a lower thermal conductivity than high RRR niobium and thus enhances the sensitivity of the calorimetry. All three pieces are joined by indium seals, which work very well at 2 K in superfluid liquid helium. Two magnetic coupling loops, the input probe and the pickup probe, are also joined with indium seals. Each of them is adjustable, using a 50- $\Omega$  transmission line brazed to an SMA connector and welded to a stainless-steel welded bellows.

The central coaxial cone is excited in the TEM mode at 1.5 GHz. The magnetic field of this mode has its maximum on the bottom surface of the cone, where the probes couple and pick up the signals. The magnetic field is circumferential and gradually decays along the cone, dropping dramatically at the open end. To have the measurement sensitivity as large as possible, a small gap of 1.5 mm has been chosen. The displacement current flowing from the center conductor to the sample, and from the sample to the conic conductor, results in a real radial current on the sample. According to our URMEL results, the maximum magnetic field on the top plate is located on a 12.5-mm-diam ring and is about 23% of its maximum value at the cone bottom. The magnetic field changes its sign at about 20 mm from the center, where the real radial current has a zero. From Fig. 2, it can be seen that when a sample's diameter is between 25.4 and 40.0 mm, the rf loss at the edge is greatly reduced, and is zero in the latter case. The outer volume of the cavity vacuum space is an antiresonant volume, which has a low field distribution and has been de-

signed to make the indium joint loss small. In addition, we have a tuning mechanism to adjust the gap, which changes the resonant frequency and can be used to shift the zero point of the field.

In our design, two factors play an important role in achieving high sensitivity. One is the tapered structure of the center part. A straight line structure, which was our initial design, had two serious disadvantages: (1) The sensitivity was at least ten times lower. (2) It was impractical to put coupling holes into the 1.5-GHz cavity if we wanted to have strong enough coupling and still put the edge of a 25.4-mm-diam sample outside of the strong field region. By using the tapered structure, we have the length of the center line reduced from 50 to 35 mm at the same resonant frequency. The rf losses along the center coaxial line, comprising 94% of the total rf losses, are thus reduced substantially. The electric field at the small end of the line is enhanced, so that there is a larger surface magnetic field on the sample. In the meantime, the arrangement of the coupling ports becomes trivial in the design as shown in Fig. 1. Another factor is the gap between the center line tip and the cavity top plate surface. The electric field decreases dramatically with increasing gap in this region, so we have to have a small gap to maintain high sensitivity. We chose a 1.5-mm gap as our design value, which becomes 1.0 mm when a 0.5-mm-thick sample is put in. In order to get this gap after electron beam welding and chemical etching, much care and attention to detail is required in the design and machining of the cavity. We chose 1.6 mm as the thickness of the top plate of part II to provide a high-temperature gradient on the top plate. These objectives have been achieved as will be described in the following section.

The geometry factors of the 25.4-mm-diam sample and of the triaxial cavity have been calculated with URMEL. They are 5682 and 44  $\Omega$ , respectively. If the sample and the cavity are made of the same material, the ratio of both losses is 0.77%, compared to 1.32% for the  $\lambda/4$  TEM cavity.<sup>3</sup>

Due to the complicated structure and the strict cleaning requirement, the cavity was assembled in several steps. Parts were first machined, then chemically polished, and then welded. Then the cavity was further machined to reach the final dimensional specifications. After all of the welding was complete, the cavity was chemically polished in a 1:1:1 solution of phosphoric acid, nitric acid, and hydrofluoric acid for 1 min. It was then rinsed in de-ionized water for several hours to rinse off the acid residue. Before assembling it in a clean room, it was ultrasonically rinsed in de-ionized water for several times in two to three hours and again in high-purity methanol for half an hour. The total thickness removed by etching is about 100  $\mu\text{m}$ .

### III. EXPERIMENTAL RESULTS

Both the cavity and the sensor chamber are under vacuum when the measurement is performed. The cavity and the sensor chamber are prepumped with a turbopump and then with two separate ion pumps. The pumping speeds of the ion pumps are 20 and 11  $\ell/\text{s}$ , respectively. At room

temperature, the vacuum before cooling is usually  $3.0 \times 10^{-7}$  Torr for the cavity and  $2.0 \times 10^{-6}$  Torr for the sensor chamber. The latter is poorer because the GE varnish we used for glueing temperature sensors has a large gas desorption rate. The vacuum readings at the pumps for both chambers at 2.0 K are in the low  $10^{-8}$  Torr range, due to the cryopumping effect. We have found that the cavity pressure before cooling is very critical because the adsorbed gas layer formed during cooling of the cavity top plate causes multipacting between the top plate and the tapered cone tip. The poorer the vacuum before cooling, the longer the time it takes, using heavily coupled rf power, to process it. Our temperature sensors have actually recorded the process of the multipacting barrier and its disappearance.

The room-temperature rf test is done with a network analyzer (HP85047A). The transmitted signal is used to measure the resonant frequency and quality factor  $Q$ . The resonant frequency is 1523.7 MHz when both the cavity and the cryostat are in vacuum and 1499.4 MHz when the evacuated cavity is in a 730-Torr cryostat. The frequency change due to pressure is about 33.3 kHz/Torr, because both the top and the bottom of the cavity are intentionally thin (1.6 mm thick). The unloaded  $Q_0$  is about 1600. From the room-temperature conductivity of niobium,  $8.0 \times 10^6$  ( $\Omega/\text{m}$ )<sup>-1</sup>, we get the geometry factor of  $G = Q_0 \times R_s = 1600 \times 27.2 \text{ m}\Omega = 43.5 \Omega$ . This agrees well with our calculated geometry factor of 44  $\Omega$ .

The cold test is done in Dewar 1, one of eight cryostats used for cavity testing and other activities at CEBAF.<sup>6</sup> It is cooled by a closed-cycle cryogenic system which can reach 1.5 K. We chose 2 K as our working temperature because the carbon composition resistors are very sensitive in this region and the BCS surface resistance of niobium is small. The pressure of the cryostat is regulated by a stepping motor controlled VAT valve. The temperature fluctuation at 2 K is less than 2 mK, which is measured both by our carbon composition resistors and by a calibrated Lakeshore germanium resistor sensor (GR-200A-500). Dewar 1 has an inner diameter of 41 cm and a depth of 183 cm. Its usable volume is 136  $\ell$ , which can last for about 12 h before refilling. This is more than enough for pumping down to 2 K, doing calibration of the carbon resistor sensors for each run, and measuring rf losses at different couplings and different field levels. The cryostat was magnetically unshielded at the time when the experiment was conducted. The lack of shielding caused a low  $Q$  due to the trapped magnetic flux, which made rf losses in the whole cavity distributed quite uniformly.

rf measurement at 2 K is done with a manually controlled system in which phase, frequency, and amplitude can be adjusted. The system uses a VCO/amplifier circuit which is phase locked to the cavity being measured. Incident, reflected, and transmitted power are measured with an HP 436A power meter, with which we can derive the power loss  $P_{\text{loss}}$  within the cavity and the coupling factor  $\beta_1$  of the input probe. We can calculate  $Q_0 = \omega\tau(1 + \beta_1)$  by measuring the resonant frequency  $\omega$  with a HP 5342A frequency counter and the decay time constant  $\tau$  with an

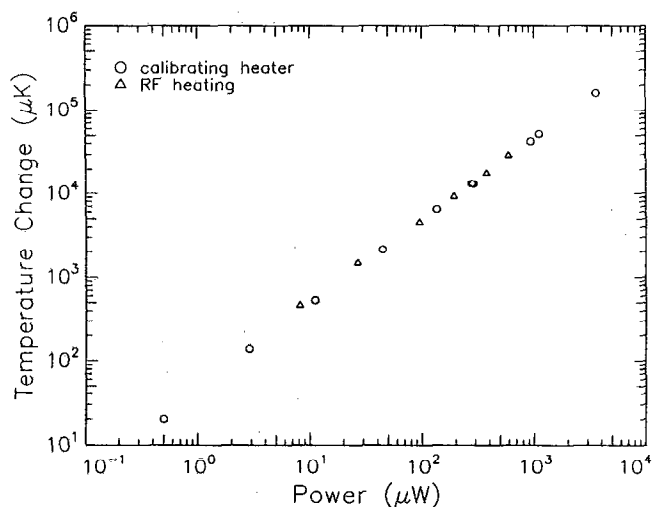


FIG. 3. Temperature change due to calibration heater (O) and rf heating ( $\Delta$ ): residual resistance induced by magnetically trapped flux dominates the loss mechanism over a wide range of rf power losses.

oscilloscope. The maximum fields in the cavity can be derived from  $U = C_1 E_{\max}^2 = C_2 H_{\max}^2 = Q_0 P_{\text{loss}}$ , where  $C_1$  and  $C_2$  are constants determined by URMEL calculations.

The unloaded  $Q_0$  of the cavity at 2 K was  $2 \times 10^7$ . From  $R_s = G/Q$ , one finds a surface resistance of  $2.2 \mu\Omega$ . The result from the calorimetric method, which measures the temperature change due to rf heating, also gave the same value. The relatively large surface resistance was caused by the magnetically trapped flux in the unshielded cryostat.

In Fig. 3, two sets of data are shown. One is the temperature sensor response to rf losses on the niobium plate, where the dissipation is determined from  $P_{\text{loss}}$  and the assumption that  $R_s$  is the same on the end plate as in the remainder of the cavity. The other is the response to a calibration heater. The heater was a 1.27-cm i.d., 1.46-cm o.d. niobium tube wound with constantan wire, which was placed on the plate center of the cavity side in the following run, with the same set of sensors at the same locations. It was used to determine the thermal conduction of the top plate, i.e., the thermal conductivity and the thickness of the plate. The heating power was measured with a Keithley 224 Programmable Current Source and a Keithley 196 System DMM. The error range of the calibration data was

generally smaller than 2%, with the exception of 5% for the lowest power point. The two curves are consistent over a substantial range of rf losses. The good agreement between the two curves suggests that the rf losses of the cavity are dominated by residual resistance caused by magnetically trapped flux. We actually calculated the magnetic field inside the cryostat from the residual resistance before we mapped it. Our estimation of the field was about 5 G. The mapping results turned out to be between 4 and 8 G, depending on the probe position. A magnetic shield and compensation coil have been added since this measurement and will be used for further measurement of high  $T_c$  superconducting thin films.

The rf losses on a top plate of  $2.2\text{-}\mu\Omega$  surface resistance is about  $711 \mu\text{W}$  at a maximum field of 95 G. Our calibration experiment determined a detection limit of  $0.05 \mu\text{W}$ . This means we can measure  $0.15\text{-n}\Omega$  surface resistance at 95 G. At the maximum field of 250 G we have reached so far, our detection limit is  $0.02 \text{ n}\Omega$ . This is much higher sensitivity than needed to measure the surface resistance of any existing material.

In conclusion, we have designed a new type of superconducting niobium triaxial cavity for surface resistance measurements. Using a 25.4-mm disk sample, this design greatly reduces edge losses and substrate interface losses of thin-film samples. By measuring calorimetrically, extra losses due to indium joints can be avoided. An extremely low detection threshold for surface resistance,  $0.02 \text{ n}\Omega$  for a 25.4-mm sample, can be achieved.

## ACKNOWLEDGMENTS

We would like to thank L. Turlington for overseeing the machining work and J. Brawley for the  $e$ -beam welding. J. Susta and other colleagues handled all the cryogenic operations. Help from L. Doolittle, P. Kneisel, P. Kushnick, G. Myneni, V. Nguyen, and C. Reece are highly appreciated. This work was supported by the U.S. Department of Energy under contract DE-AC05-84ER40150.

<sup>1</sup>N. Klein, Proceedings of the Fifth Workshop on rf Superconductivity, edited by D. Proch, DESY M-2-92-1, 285 (1992).

<sup>2</sup>A. M. Potis, D. W. Cooke, and E. R. Gray, J. Supercon. 3, 297 (1990).

<sup>3</sup>J. R. Delayen, C. L. Bohn, and C. T. Roche, Rev. Sci. Instrum. 61, 2207 (1990).

<sup>4</sup>T. Weiland, IEEE Trans. Nucl. Sci. NS-32, 2738 (1985).

<sup>5</sup>K. Halbach and R. F. Holsinger, Part. Accel. 7, 213 (1976).

<sup>6</sup>C. Reece, J. Susta, T. Powers, and B. Almeida, 1991 IEEE Particle Accelerator Conference 4, 2325, (1991).